Space Lidar Developed at the NASA Goddard Space Flight Center—The First 20 Years

Xiaoli Sun, *Member, IEEE*, James B. Abshire, *Senior Member, IEEE*, Jan F. McGarry, Gregory A. Neumann, James C. Smith, John F. Cavanaugh, David J. Harding, H. Jay Zwally, David E. Smith, and Maria T. Zuber

***Abstract*—During the past 20 years the NASA Goddard Space Flight Center has developed five different lidar for space, and has successfully used them in orbital missions to map Mars, the Earth, the Moon and Mercury. Although similar in some ways, each of these lidar has had a different combination of measurement requirements, payload constraints, and operational environments. Together they have improved space-based laser measurement technologies and advanced planetary science. This paper gives a brief overview of these instruments, their measurement approaches and designs, and some highlights from their scientific observations.**

***Index Terms*—Laser altimeter, lidar.**

I. Introduction

LIDAR measurements from orbit provide a unique and powerful tool for monitoring the Earth's environment and exploring the planets. Because of the shorter wavelengths, lidar can focus the energy into much narrower beams and achieve higher spatial resolution with a smaller transmitter than radar. Since lidar utilize their own source of illumination, they can provide continuous measurements both day and night, including over polar-regions in darkness where passive instruments cannot observe. Individual lidar measurements can be accurately located horizontally at a scale comparable to the laser beam footprint size. Using short laser pulses allows the lidar receivers to determine range and, consequently, surface elevation at centimeter to decimeter precision, which is much more accurate than measurements from radar and stereoscopic imaging.

During the past 20 years, the NASA Goddard Space Flight Center (GSFC) has successfully developed five space lidar instruments. They were the Mars Orbiter Laser Altimeter (MOLA) on the Mars Observer [1] and Mars Global Surveyor (MGS) missions [2]–[4], the Geoscience Laser Altimeter System (GLAS) on the Ice, Cloud, and land Elevation Satellite (ICESat) mission [5]–[9], the Mercury Laser Altimeter (MLA) [10] on the MErcury Surface, Space ENvironment, GEochemistry, and Ranging (MESSENGER) mission [11]–[14], and the Lunar Orbital Laser Altimeter (LOLA) [15], [16] on the Lunar Reconnaissance Orbiter (LRO) mission [17]. They all used Q-switched Nd:YAG laser transmitters that were diode pumped and emitted 5 to 8 ns wide pulses at 1064 nm at rates from 8 to 40 Hz. The GLAS laser also used a frequency-doubling crystal to split part of the laser energy to 532-nm wavelength for more sensitive atmospheric backscatter measurements.

The lidar receivers used telescopes that were co-aligned with the laser beam and had fields of view (FOV) a few times larger than the laser divergence angle. All these lidar receivers used direct detection and silicon avalanche photodiode (APD) detectors. In addition to estimating range, they also collected the transmitted and the received laser pulse energy and pulsewidth to provide information about the surface slope, roughness, and reflectance.

Each of these lidar projects experienced its own technical challenges due to the payload constraints, operating environment, and measurement requirements. Each also resulted in a major advancement in measurement capability, instrument size, mass, power, and space operation environment, for which GSFC has gained valuable knowledge and experience in space borne lidar applications. Two of these lidar, MLA and LOLA, are still operating in orbit as of this publication. Table I gives a summary of the timelines, the primary science measurements, and major achievements of these lidar. Table II lists the main characteristics of these five lidar. In this paper, we give a brief review of each of these instruments, the technologies and sample measurement results, and look ahead to future projects.

II. MOLA on the Mars Observer and MGS Missions

The Mars Orbiter Laser Altimeter (MOLA) was one of six science instruments on the Mars Observer mission that was launched in 1992 [1]. MOLA's major objective was to map the topography of Mars, both its global shape and local features, for one Martian year. MOLA was the first space lidar developed using a diode-pumped Nd:YAG laser. Using the newly available AlGaAs laser diode arrays as pumps for the laser slab allowed the laser to be smaller, more rugged, and much more efficient in converting electrical to optical power. For the first time this allowed a space laser to be small and conductively cooled, operate at pulse rates >1 Hz and has a lifetime of >1 year [18]. Tests performed during cruise phase showed that

Manuscript received September 30, 2012; revised January 09, 2013, March 07, 2013; accepted April 12, 2013. Date of publication May 30, 2013; date of current version June 17, 2013.

X. Sun, J. B. Abshire, J. F. McGarry, G. A. Neumann, and D. J. Harding are with Solar System Exploration Division, Goddard Space Flight Center (GSFC), National Aeronautics and Space Administration (NASA), Greenbelt, MD 20771 USA (e-mail: xiaoli.sun-1@nasa.gov).

J. F. Cavanaugh and J. C. Smith are with the Instrument Systems and Technology Division, Goddard Space Flight Center (GSFC), National Aeronautics and Space Administration (NASA), Greenbelt, MD 20771 USA.

H. J. Zwally is with the Earth Science Division, Goddard Space Flight Center (GSFC), National Aeronautics and Space Administration (NASA), Greenbelt, MD 20771 USA.

D. E. Smith was with the Solar System Exploration Division, Goddard Space Flight Center (GSFC), National Aeronautics and Space Administration (NASA), Greenbelt, MD 20771 USA. He is now with Department of Earth, Atmospheric and Planetary Science (EAPS), Massachusetts Institute of Technology (MIT), Cambridge, MA 02139 USA.

M. T. Zuber is with the Department of Earth, Atmospheric and Planetary Science (EAPS), Massachusetts Institute of Technology (MIT), Cambridge, MA 02139 USA.

Color versions of one or more of the figures in this paper are available online at http://ieeexplore.ieee.org.

Digital Object Identifier 10.1109/JSTARS.2013.2259578

TABLE I
SUMMARY OF THE TIME LINES, SCIENCE MEASUREMENTS, AND MAJOR ACHIEVEMENTS OF THE SPAC LIDAR DEVELOPED AT NASA GSFC

Instrument	**MOLA**	**GLAS**	**MLA**	**LOLA**
Mission	MO & MGS	ICESat	MESSENGER	LRO
Planet	Mars	Earth	Mercury	Moon
Years in space	1992-1993, MO 1996-2006 MGS	2003-2010	2004-present	2009-present
Science and Engineering Highlights	First orbiting planetary laser altimeter	First Earth orbiting precision laser altimeter and atmosphere lidar	MOLA like but ~1/5 the size, 3-4 times maximum range, 1/3 the ranging precision	First multibeam space laser altimeter, MLA-like but with 5 beams
Science Measurements	Topography, global shape, gravity, and local surface features, cloud height and distribution	Rate of change of icesheets, land topography, vegetation height, atmosphere backscattering profiles at dual wavelength	Topography, global shape, gravity, local surface features, reflectanc of volatiles in permenant shadowed craters	Topography, global shape, gravity, local surface features reflectance of volatiles in permenant shadowed craters
Orbit Altitude	400 km	600 km	200-15,000 km	30-200 km
Maximum range	800 km	>>600 km	1600 km	170 km
Global measurement accuracy	0.7 m radial, 100 m horizontal	1 cm radial, 70 m horizontal	1 m radial, 100 m horizontal	1 m radial, 50 m horizontal
Precision (single shot)	25 cm	2.0 cm	15 cm	10 cm
Measurement rate	10 Hz	40 Hz	8 Hz (~7% duty cycle)	28 Hz x 5 beams
laser shots fired	670 million	2 billion	19 million (as of 12/31/2012)	2.7 billion (as of 12/31/2012)

TABLE II
COMPARISON OF THE CHARACTERISTICS OF THE SPACE LIDAR DEVELOPED AT NASA GSFC

Instrument	**MOLA**	**GLAS**	**MLA**	**LOLA**
Laser design	Diode pumped Nd:YAG, active q-switched, 1 stage (power oscillator)	Diode pumped Nd:YAG, passive q-switched, 3-stages oscillator+preamplifier +power amplifier	Diode pumped Nd:YAG, passive q-switched, 2-stages oscillator+preamplifier	Diode pumped Nd:YAG, passive q-switched, 1-stage (oscillator only) 5-way beam split via a DOE
Number of lasers	1	3	1	2
Wavelength	1064 nm	1064 and 532 nm	1064 nm	1064 nm
pulse energy	45 mJ	75 mJ 1064nm, 35 mJ 532nm	20 mJ	3 mJ
Beam quality	multimode	quasi single mode	single spatial mode	single spatial mode
Divergence	0.37 mrad	0.11 mrad	0.08 mrad	0.1 mrad
Receiver Telescope	50 cm diameter, Be Cassegrain	100 cm diameter, Be Cassegrain	12 cm diameter, 4 each Sapphire lenses, fiber coupled	15 cm diameter, BK7 lens, fiber coupled
Receiver Field of view	0.85 mrad	0.5 mrad	0.4 mrad	0.4 mrad
Receiver optical filter	2 nm	0.8 nm (0.03 nm for 532 nm)	0.8 nm	0.8 nm
Detectors	Si APD, analog	1064 nm: Si APD, analog 532 nm: Si APD Single photon counting	Si APD, analog	Si APD, analog, one detector per beam
Pulse measurements	pulse rise time, width, and energy	full pulse waveforms at 1Gs/s	pulse rise times and widths at 2 thresholds	pulse rise times and widths and energy
Timing resolution	2.5 nsec	<0.1 nsec (pulse waveform centroid)	0.4 nsec	0.17 nsec
Receiver Clock stability	<1e-7/day	<1e-9/day	<1e-7/day	<1e-12/day
On board science algorithm	automatic detection threshold adjustment, range gate control, ground echo histogram and tracking.	maximum likelihood signal detection, cloud rejection, automatic detector gain control, range gate control, automatic etalon filter temperature control.	automatic detection threshold adjustment, range gate control, detector gain adjustment, ground echo histogram and tracking.	automatic detection threshold adjustment, range gate control, ground echo histogram and tracking.
Mechanisms	none	4	none	none
Thermal control approach	heaters and thermostats	Loop heat pipes (LHP), 3 sets	heaters and thermostats	heaters and thermostats
Data rate	0.51 kbit/sec	300 kbit/sec	0.5 kbit/sec (average)	28 kbit/sec
Average Electrical Power	31 W	300 W	17 W	34 W
Mass	26 kg	300 kg	7.4 kg	12.5 kg
Size	0.7 x 0.7 x 0.5 m	1.0 x 1.4 x 1.8 m	0.28 x 0.28 x 0.26 m	0.35 x 0.35 x 0.29 m

MOLA performed well prior to Mars orbit insertion. Unfortunately, the Mars Observer mission ended prematurely in August 1993 due to a spacecraft failure while preparing for orbit insertion.

Two similar space lidar were subsequently developed by other institutions with principal science participation from NASA GSFC. These were the Laser Altimeter on the Clementine mission to the Moon [19], [20] developed by the Naval

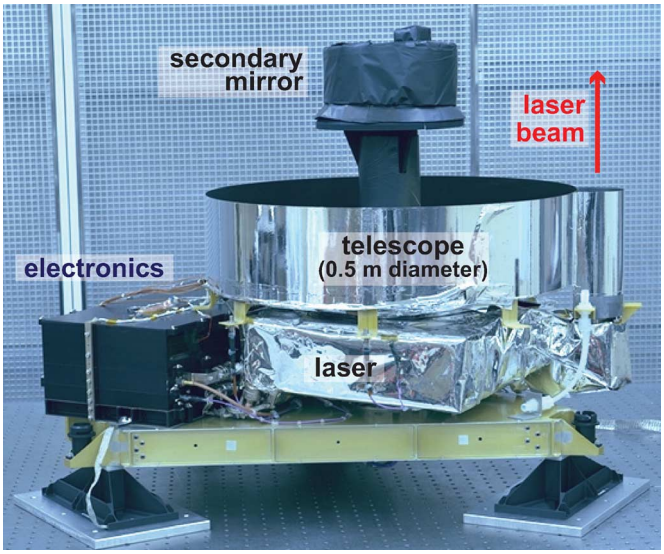

Fig. 1. Photograph of MOLA at NASA GSFC prior to delivery to the MGS spacecraft.

Research Laboratory, and the Laser Rangefinder on the Near Earth Asteroid Rendezvous (NEAR) mission to Asteroid 433 Eros [21], [22] developed by the Johns Hopkins University Applied Physics Laboratory (JHU-APL).

A second version of MOLA was built between 1994 and 1996 and launched in 1997 on board the Mars Global Surveyor (MGS) [2]–[4]. It used the same design approach as the first MOLA, but included upgrades in the laser and the receiver electronics. Fig. 1 shows a photograph of MOLA prior to delivery to the MGS spacecraft, and Fig. 2 shows its block diagram [23]. The basic approach to MOLA was adapted from previous experience with airborne laser altimeters development at NASA GSFC [24]. It consisted of an actively Q-switched Nd:YAG laser that was similar to lasers originally developed for target designators and for free space laser communications [18]. The laser was physically mounted between the telescope and the base plate with the laser beam emitted at the side of the receiver telescope, as shown in Fig. 1. The details of the instrument's opto-mechanical design and calibration is summarized in [25].

MOLA used a direct detection receiver with a 50 cm diameter beryllium Cassegrain telescope, a silicon APD detector, and an electronics assembly using 4 parallel signal processing channels. The MOLA telescope was adapted from ones used on the Infrared Spectrometer (IRIS) for the Voyager mission and the Composite Infrared Spectrometer (CIRS) on the Cassini mission. The silicon APD detectors were originally developed for a free-space laser communications program, and had enhanced quantum efficiency (up to 40%) at 1064-nm wavelength [26]. The detector output was fed to a bank of four low-pass filters and comparators in parallel and a time interval unit (TIU), as shown in Fig. 2. Because the terrain on Mars was known to vary considerably in slope and roughness, the echo pulsewidth was expected to vary widely. The design approach used four matched filters in parallel to maximize the probability of a successful range measurement. The four low-pass filters had Gaussian impulse responses with widths of 20, 60, 180, and 540-nsec full-width-at-half-maximum (FWHM) to span the range of expected ground echo pulse shapes [23]. The output of the first filter that exceeded its detection threshold stopped the TIU. Due to the delay times of the filters, this favored the fastest response channel with a strong signal when more than one channel was triggered.

The receiver threshold levels were automatically and independently adjusted by an algorithm in the MOLA flight computer to maintain a false-alarm rate of approximately 1% per channel per range gate interval under any solar background conditions. Each receiver channel contained a noise counter that monitored the rate of the noise threshold crossings for the threshold control loop. Each MOLA receiver channel also had a range gate. The range gate eliminated false triggers outside the expected target range interval and allowed the receiver to further lower its detection threshold and improve the receiver sensitivity. Another on-board algorithm tracked the ground returns and centered the range gate at the expected target range. The algorithm also adjusted the range gate width according to the dynamics of the surface topography. Finally, the algorithm automatically switched the receiver between acquisition and tracking modes based on a set of success criteria for target detection.

The second MOLA receiver used a field programmable gate array (FPGA) to perform most of the digital signal processing. This allowed room for a time-interpolator circuit that used a tapped-delay-line technique to improve the receiver's timing resolution from one clock period, 10 nsec (1.5 m in range) to 2.5 nsec. An oven controlled crystal oscillator (OCXO) was used that had better than 10^{-9} short term stability. The MOLA receiver also recorded the leading edge times of the received pulses, the pulse width, and integrated the pulse energy in between the two threshold crossings [23]. Assuming a Gaussian pulse shape, the pulse width, amplitude, and arrival time could be uniquely solved from those measured at the threshold crossings and the threshold value in the telemetry. The measured pulse widths were also used to correct for the time shift, or "time-walk" of the receiver's threshold crossing time due to signal amplitude fluctuations. The pulse energy measurements were used to estimate the product of two-way atmospheric transmission and surface reflectance. In addition MOLA software measured the time difference between the spacecraft mission elapse time (MET) and that of its own clock oscillator at 4-msec resolution to reference the laser pulse emission time to MET and to estimate the MOLA clock frequency against the spacecraft ultra-stable oscillator (USO) frequency that was monitored from ground via the radio frequency (RF) link. These enabled merging of MOLA ranging data measurements with the spacecraft's pointing and position information to accurately geolocate the laser footprint on the surface to within 100 m.

MOLA on MGS collected 671 million Mars surface topographic measurements. These included intermittent operations during a 17-month MGS aerobraking period in highly elliptical orbits. During this period, the spacecraft relied on drag from the Martian upper atmosphere at periapsis to reduce the orbital velocity in order to circularize the orbits. The elliptical orbits gave the MOLA team an opportunity to assess the instrument's capability at different altitudes. Once the orbit was circularized, MOLA provided continuous range measurements

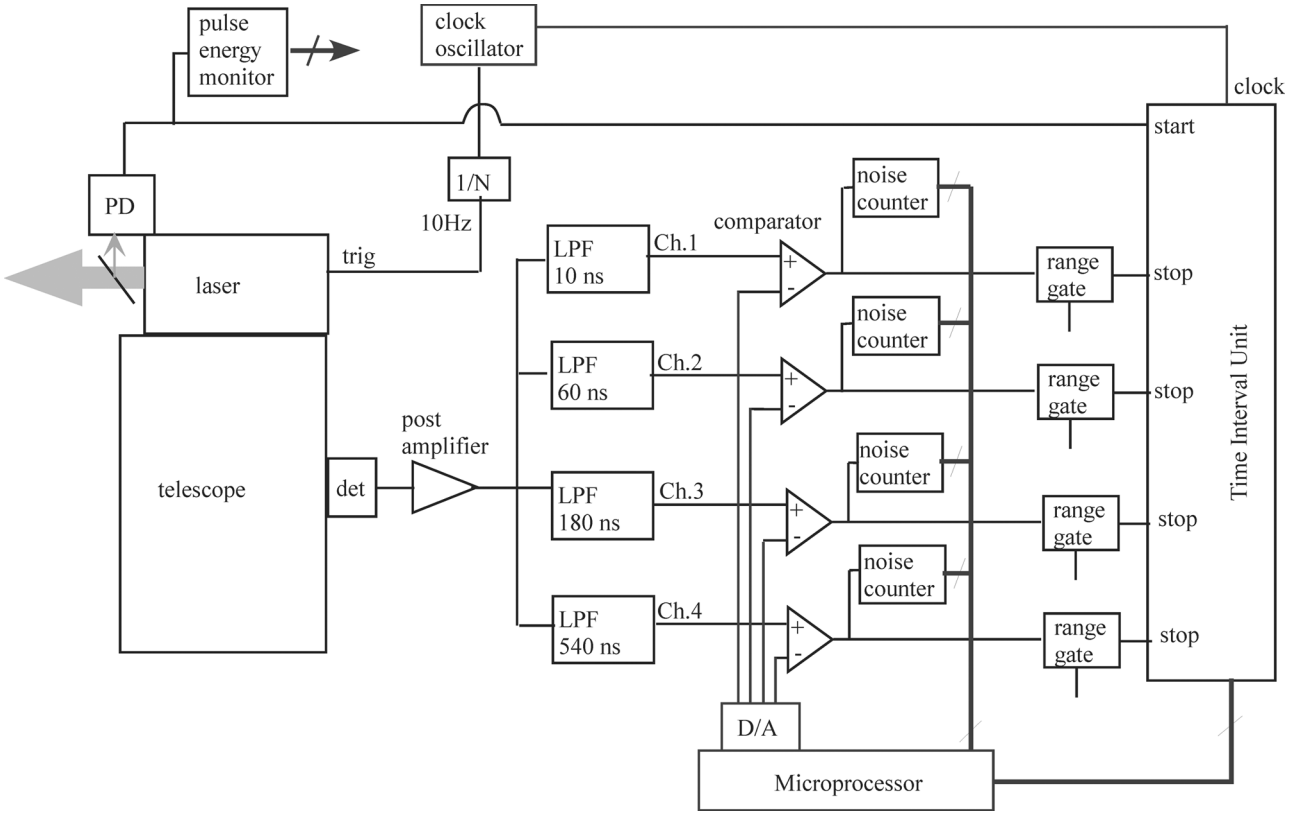

Fig. 2. Block diagram of MOLA [23].

for 27-months (1.12 Martian year) at 400 km altitude [2]–[4]. The ranging precision was about 40 cm [27]. The absolute range accuracy was limited by uncertainties in the spacecraft orbital position and altitude determination, which was about 1 meter in the radial direction and a few hundred meters in spatial position. Fig. 3 shows a Mars topographic map produced by interpolation of MOLA elevation measurements [4]. MOLA also provided surface slope and roughness measurements from the pulsewidth [27] and surface reflectance from the received pulse energy. In addition, MOLA detected clouds, some of which produced strong echoes and allowed a height measurement. Thin clouds and dust that did not produce a detectable range signal gave a measure of the atmosphere transmission when compared to the signals measured through a clear atmosphere [28].

It was found during the MOLA science measurements that the receiver false trigger rate and the detection threshold setting in the telemetry could be used to solve for the scene-reflected solar background illuminating the detector. This allowed the MOLA receiver to be used as a passive 1064-nm radiometer to measure the daytime "scene brightness" within the receiver FOV and hence the Mars surface reflectance and atmosphere scattering under solar illumination [29]. After MOLA suffered a clock oscillator failure and lost its ability to trigger the laser, the instrument continued to operate for passive radiometry measurements through the end of the MGS mission in 2006. These passive radiometry measurements were unique since they were over a narrow spectral range, 1064 ± 1 nm, and every pixel was geolocated to the same accuracy and precision as the topography measurements. Fig. 4 shows a series of Mars polar maps over different seasons and the corresponding changes of the ice cap sizes from the MOLA passive radiometry measurements [30].

III. GLAS on the ICESat Mission

The Geoscience Laser Altimeter System (GLAS) on the Ice, Cloud, and land Elevation Satellite (ICESat) mission was developed at NASA GSFC as the first operational Earth orbiting lidar. The primary science objectives of the ICESat mission were to monitor changes in the ice-sheet elevations of Antarctic and Greenland [5]. In order to meet its science objectives, the GLAS lidar was designed to have <10 cm single shot precision and <1 cm accuracy after averaging over a 200×200 km area. These required a substantially higher performance lidar than for MOLA [7]. The major technical challenges for GLAS were to achieve the required measurement accuracy, long-term ranging stability, lifetime, laser pointing angle determination, and to profile atmospheric backscatter at both 1064 and 532 nm. During the time of its development, two pathfinder Shuttle Laser Altimeters (SLA) experiments were flown, one on STS-072 in 1996 and the other on STS-085 in 1997 [31]. The SLA experiments used the MOLA engineering model laser, detector, and electronics, and added an analog to digital converter (ADC) to record the pulse waveforms. The SLA experiments first demonstrated the capability for a space-based lidar to measure the Earth's land, ocean, and vegetation canopy heights.

Fig. 5 shows a photograph of GLAS on the ICESat spacecraft [8]. GLAS carried three identically-designed diode-pumped Q-switched Nd:YAG lasers, with one primary and two spares [32]. The passively Q-switched lasers had 3 stages, and emitted

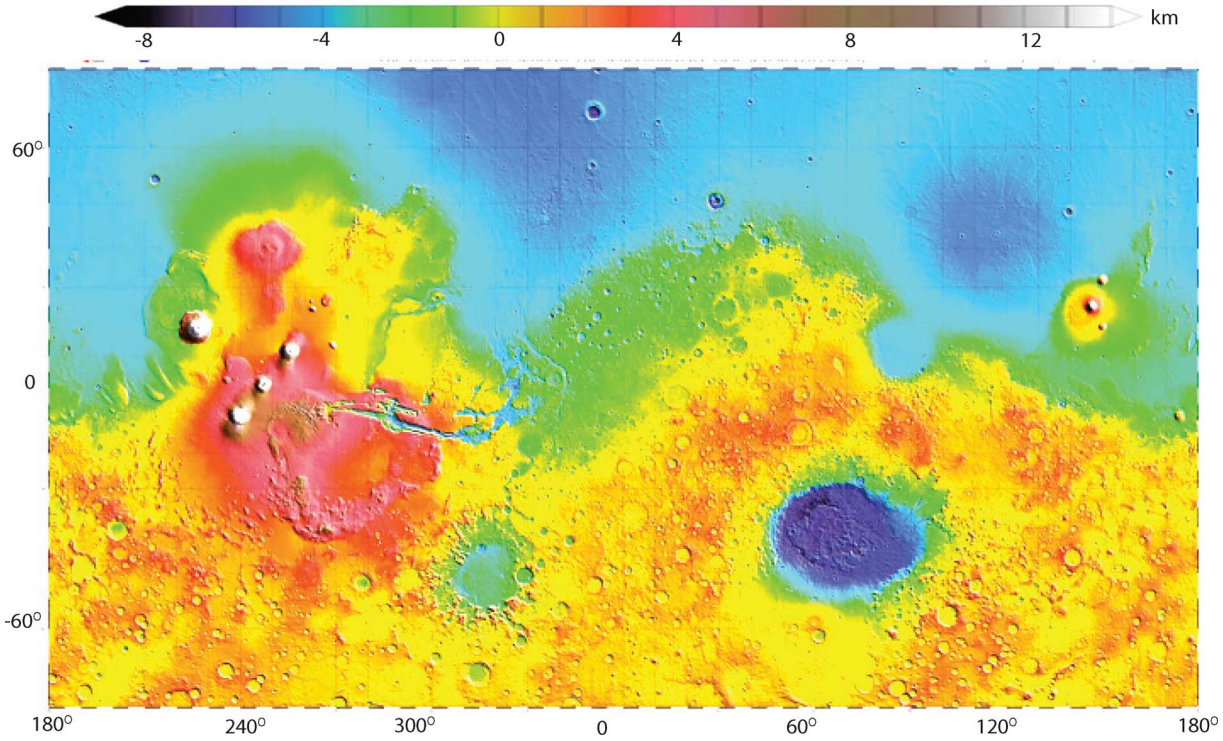

Fig. 3. Mars topographic map from 671 million MOLA measurements [4].

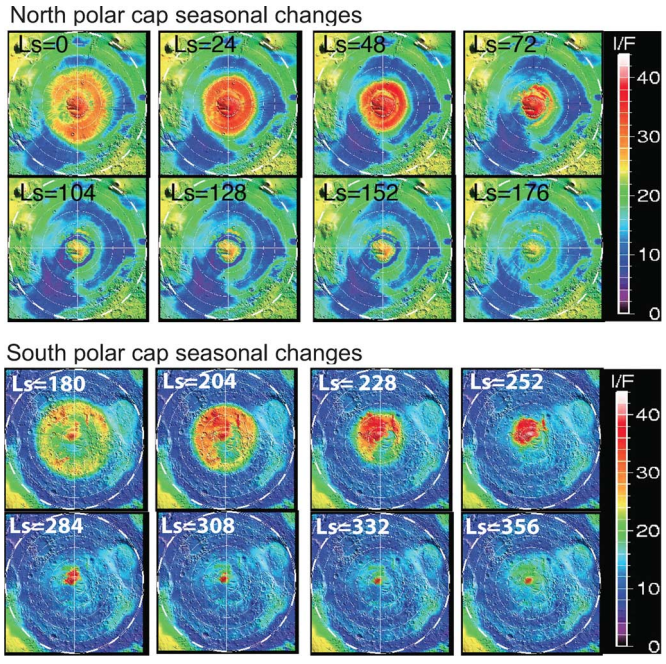

Fig. 4. Maps of Mars polar region surface reflectance to sunlight, showing seasonal changes of the ice caps at the poles. The label "Ls" refers to the solar latitude, which is the position of Mars in its orbit around the Sun, with $\mathrm{Ls} = 0°$ corresponding to the vernal equinox [30].

6-nsec wide pulses at 1064 and 532 nm at a 40-Hz pulse rate. The output beam produced a nominally single-lobed far-field pattern so that variability of the surface height could be inferred from the received pulse shape. To measure the laser pointing angle, GLAS also employed a Stellar Reference System (SRS) [33], which folded back a small fraction of the laser beam onto a star camera, with the use of a lateral transfer retro-reflector (LTR), and was able to monitor the laser pointing angle to a few arcseconds relative to the star field. The on-board Global Position System (GPS) receiver measured the spacecraft position to 2–3 cm accuracy. Fig. 6 shows a block diagram of the instrument.

GLAS lasers had 100-μrad divergence angle. The receiver used a 1-m diameter telescope with a 500-μrad receiver FOV. This was chosen to minimize noise from solar background light while maintaining bore-sight. GLAS used a silicon APD detector for the 1064-nm channel, like the one used in MOLA, but with an improved preamplifier circuit. The GLAS detector assembly had a wider bandwidth, nearly linear phase response and wider linear dynamic range [26], [34]. The GLAS receiver also used a waveform recorder that sampled at a 1-GHz rate the transmitted and received pulse waveforms. The laser pulse time-of-flight was determined in data analysis via curve fits of the recorded pulse waveforms to known pulse shape functions. This approach was 2–3 times more precise than using threshold crossing times. The echo pulse waveforms also gave considerably more information about the target, including surface height, slope, roughness, and pulse spreading from vegetation within the laser footprint. The echo pulse waveforms from land surface were fit to multiple Gaussian pulse shapes to resolve ground echo and treetop canopy returns.

The GLAS altimetry receiver used a set of low-pass matched filters to optimize the likelihood of surface detection, just like MOLA. However, the low-pass filters in GLAS were implemented digitally to untilize the already-recorded digital waveform. The receiver incorporated a finite impulse response

Fig. 5. Photograph of the GLAS upon lidar integration with ICESat at Ball Aerospace and Technology Corp.

(FIR) filter chip and passed the echo pulse waveform signal through the FIR filter six times in succession while reducing the sample rate by $1/2$ each time. This series of steps effectively formed six low-pass filters in series with 4, 8, 16, 32, 64, and 128 nsec FWHM impulse responses, respectively. Onboard algorithms calculated mean and the root-mean-square (rms) noise levels from waveform segments prior to the arrival of the backscattered laser signal. The algorithm set the detection thresholds to be 5 to 7 times the rms noise to maintain a $\sim 1\%$ false detection rate within the range gate [35]. The algorithm calculated signal-to-noise ratio (SNR) as the ratio of the peak pulse amplitude to the rms noise, and selected the output of the filter with the highest SNR as the likely ground return. The pulsewidth and arrival times were also considered in addition to SNR in distinguishing the likely ground returns in the presence of clouds. It assigned a weight to each of these factors, calculated a modified likelihood function for each low-pass filter output, and selected the one with the highest likelihood. The weighting factors, the matched filter impulse response function, and the threshold values were all programmable via ground commands. After the likely ground return was found, the algorithms identified the segment of raw waveform about the ground return, 544 sample points for land and ice and 200 points for ocean surface, and downlinked these waveform segments to ground for further processing. The transmitted laser pulses were detected by the same detector and digitizer and downlinked to ground as well. The range gate location was set according to a Digital Elevation Map (DEM) of Earth stored on board. The range gate width was set according to the surface slope and the dynamics of DEM. The centroids of both pulses were also calculated on board to determine the approximate laser pulse time of flight and a histogram was calculated to determine if the receiver was properly tracking the ground.

The GLAS lidar also collected range-resolved atmospheric backscatter profiles at 1064 nm and 532 nm [36]. The 1064-nm APD's output was split into two channels, one digitized at a 1-GHz rate for surface altimetry and the other low-pass filtered and digitized at a 2-MHz rate (75-m vertical resolution) for the entire atmosphere column to 20-km altitude above the surface. These atmosphere backscatter profiles were then downlinked for further processing. The 532-nm receiver had a 160 μrad FOV and its position could be adjusted and centered on the laser signal on orbit. It used a temperature-tunable etalon with a 30-pm pass-band to reduce the effect of solar background light. The center wavelength of the etalon was tuned to the average laser wavelength via an automatic temperature control loop. The optical output from the etalon was split equally into eight Geiger-mode silicon APD single photon counting modules (SPCM) [37]. These detectors were used in parallel to prevent count rate saturation from bright scenes, such as solar illuminated clouds or snow.

From space, the GLAS altimeter channel demonstrated a ranging precision of 2.0 cm, as determined from the standard deviation of the measurements over a smooth ice-covered surface of Lake Vostok in Antarctica, as shown in Fig. 7. Similar ranging accuracy and precision were confirmed by comparing GLAS measurements with GPS survey results over Salar de Uyuni, Bolivia, over a multi-year period [38]. Fig. 8 shows a shaded relief topographic map of Antarctica and Greenland derived from the GLAS data. Fig. 9 shows the changes of Antarctic ice sheet elevation as monitored by GLAS. In addition, GLAS measured sea ice thickness in the Arctic based on its freeboard, defined as the height of the floating ice above the relatively smooth ocean surface in between the floating ice [39]. Fig. 10 shows the Arctic sea ice thickness as measured by GLAS from 2004 to 2009.

Echo-pulse waveforms from GLAS enabled sampling of forest height over the globe. Estimating the above-ground biomass is a key component in monitoring the global carbon cycle [40]. GLAS echo-pulse waveforms from vegetated landscapes were complex because of height and density variability of the canopy structure and underlying surface topography within the laser footprint [41]. In areas of low to moderate slope, where the ground echo and the canopy echoes could be uniquely resolved, the average canopy height could be reliably measured to assist in biomass estimate of the area. Fig. 11 shows a global vegetation map from a combination of *in situ* survey, GLAS measurements, and optical and microwave imagery [40].

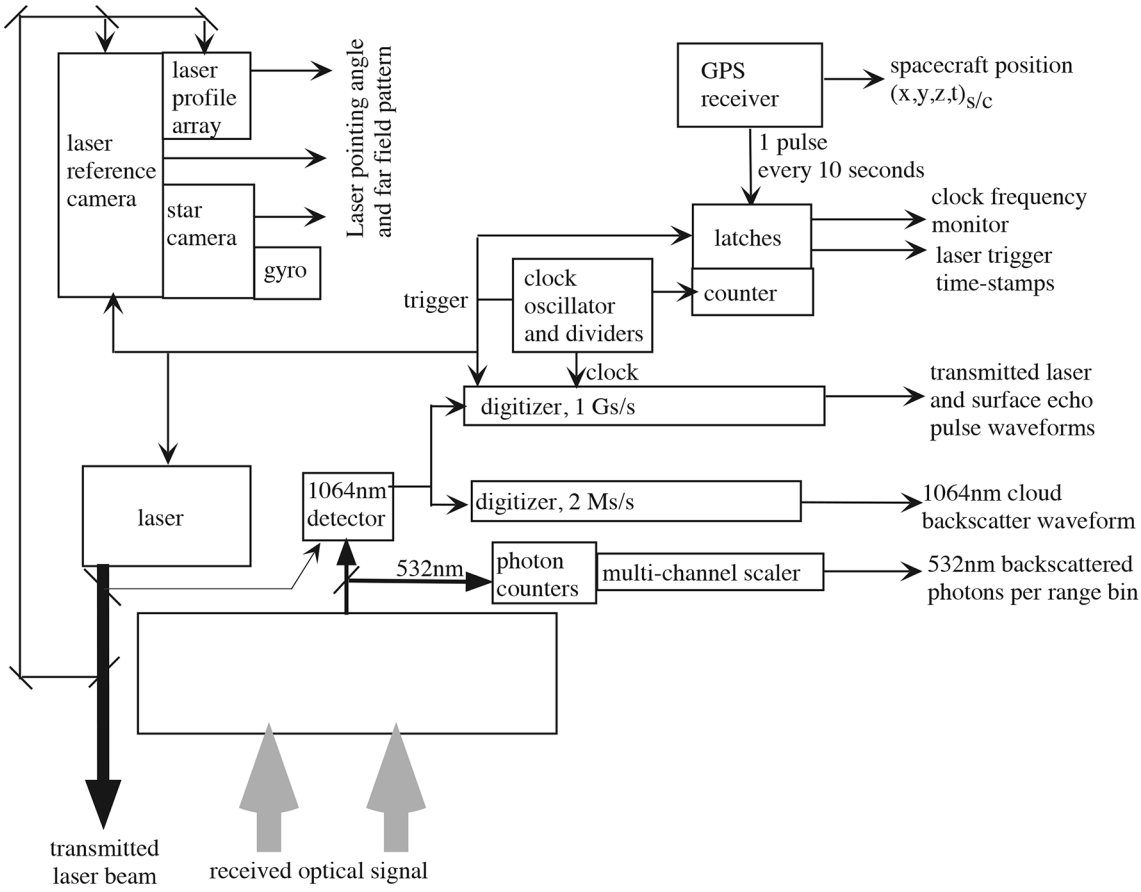

Fig. 6. Block diagram of the GLAS instrument.

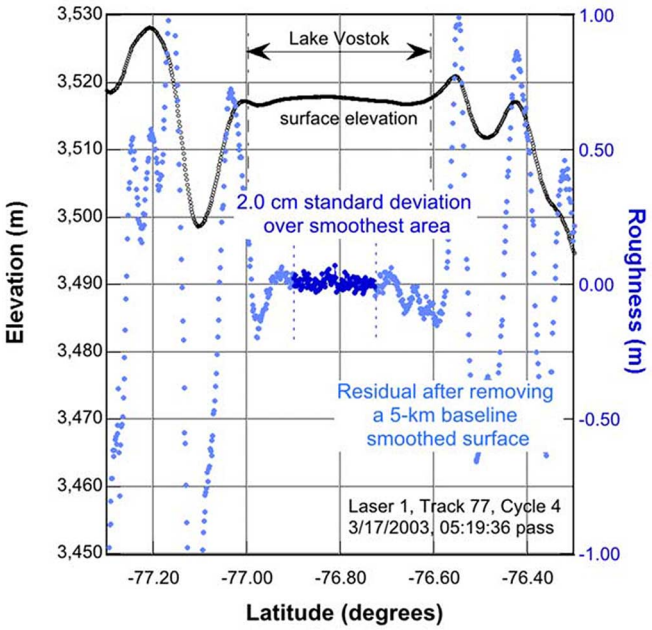

Fig. 7. Elevation profile and residual after removing a 5-km running-average baseline of Lake Vostok, Antarctic, from GLAS measurement [8].

The GLAS 1064-nm atmosphere channel was shown to detect clouds and aerosols to a cross section as low as 10^{-6}/m-sr. The 532-nm channel was about ten times more sensitive, detecting aerosol to a cross section as low as 10^{-7}/m-sr [42]. The 532-nm channel could also detect much weaker molecular backscatter at 20 to 40 km altitude with a longer integrating time. This served as a reference for the calibration of the GLAS receiver optical throughput and detector sensitivity. Fig. 12 shows an example of the GLAS atmosphere measurements.

During its 6.5-year mission in space [43] GLAS collected 1.98 billion laser measurements of altimetry and atmosphere backscatter profiles. This provided uniquely-valuable measurements for Earth climate studies and new insights for future space lidar developments. Table III shows the GLAS measurement periods over the entire mission time [43]. There were a total of 18 campaign periods that were conducted three times per year from 2003 to 2006, and twice per year thereafter, mostly with a 33-day duration. Although originally planned to operate continuously, the premature failure of the first laser and faster-than-expected degradation in the second laser led to a modification of the mission to a series seasonal measurements in order to optimize the mission duration and science observations. All of the other GLAS receiver components performed well in space for the entire mission. As expected, the silicon APD single photon detectors showed a slow and steady increase in the dark count rate in response to space radiation. This degradation was close to the rate predicted based on pre-launch ground testing. At the end of the mission the dark count rate was still lower than that of daytime solar background [36], [37].

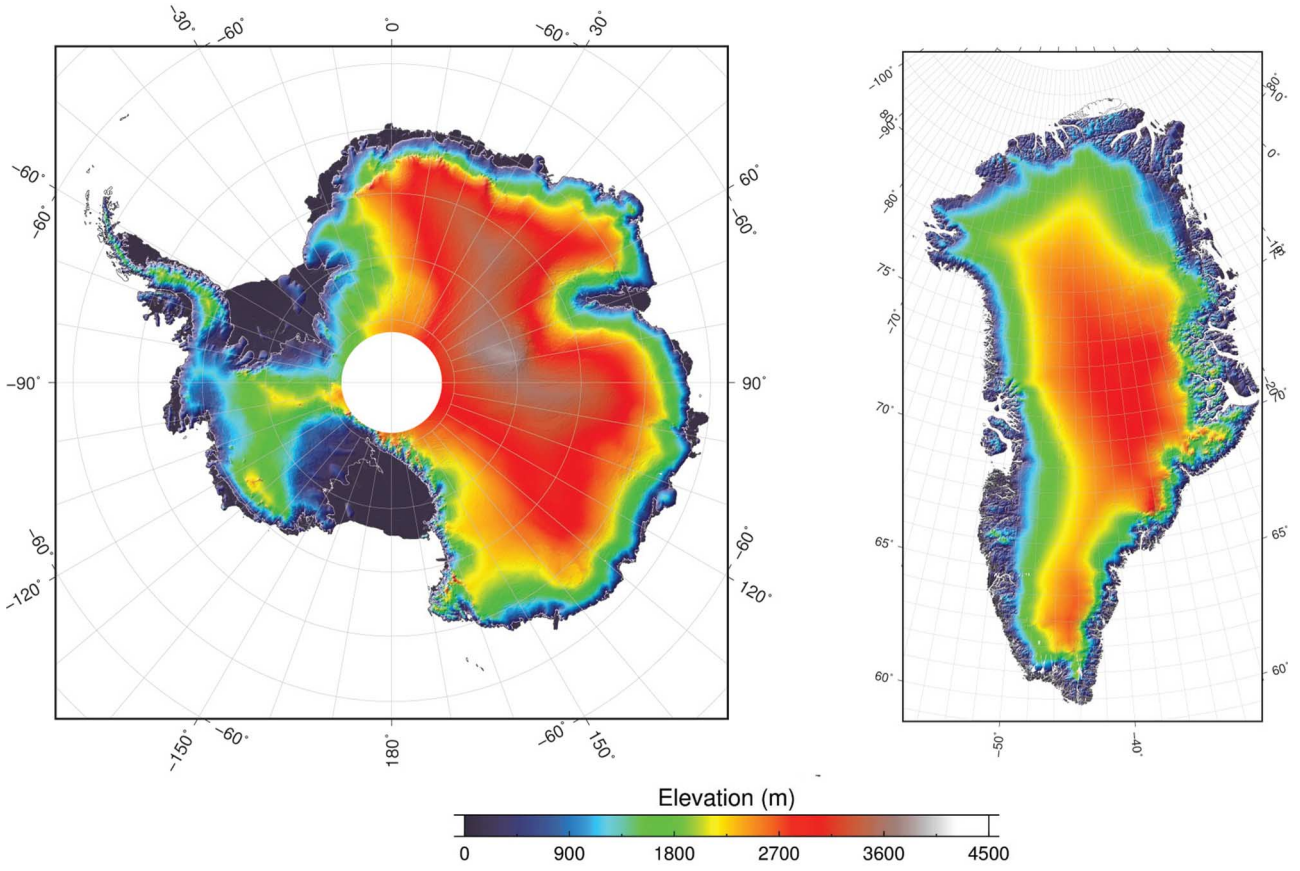

Fig. 8. Shaded relief image of Antarctic and Greenland icesheet topography measured by GLAS using similar color table and shading as in Mars topography map from MOLA.

IV. MLA on the Messenger Mission

The Mercury Laser Altimeter (MLA) is one of seven instruments onboard NASA's MErcury Surface, Space ENvironment, GEochemistry, and Ranging (MESSENGER) mission to Mercury. The primary objective of MLA is to measure the topography of the northern hemisphere of Mercury from orbit and quantify the oscillation pattern of the planet self-rotation, or libration, due to its locked spin period to rotation ratio and its eccentric orbit about the sun. The MLA instrument design was quite challenging because it had to collect range measurements from the highly elliptical orbits around Mercury with extremely tight constraints in mass, size, and power.

MLA operates in a highly variable and extreme thermal environment. Although protected from direct sunlight by the spacecraft sunshade, MLA still receives large heat flux from Mercury, whose surface temperature rises to above 700 K on the sunlit side and drops to 90 K on the dark side. Thus, MLA has to survive constant thermal cycling every orbit and thermal shock as the spacecraft travels around Mercury every twelve hours (eight hours after April 2012), crossing the terminator between the hot side and cold side in minutes. This operating environment is more severe that the vacuum test chambers at NASA GSFC could simulate [10].

To save power and mass, the MLA laser is powered on only when Mercury is within its ranging capability and the laser bench temperature is allowed to increase by as much as 20°C over a 40-minute operating period. The instrument is switched between several modes by the spacecraft: power-off (survival heaters only), Keep-alive, Stand-by, and Science, each with a different power dissipation and self-heating or cooling rate. The phasing of the instrument power states is adjusted based on thermal predictions so that the laser is always in its proper operating temperature range when Mercury is within range. Another challenge is that the laser beam has to be kept perpendicular to direct sunlight so that the sunshade of the spacecraft can face the sun at all times. As a result, range measurements are often made at a slant angle to the surface, which affects the ranging capability, measurement precision, and laser footprint geolocation. Fig. 13 shows a conceptual diagram of the Mercury and MESSENGER orbits, the MLA measurement geometry, and the thermal environment at different portions of the orbit [44]. Fig. 14 shows a photograph of the MLA instrument [10].

MLA was developed from 2001 to 2004 to be a miniaturized version of MOLA but with longer range and ability to withstand harsher operating environments [10]. The MLA laser design was largely based on that of the first two stages of the GLAS laser design with a 20 mJ/pulse energy and 8 Hz pulse rate [45]. The laser had a single spatial mode and was collimated to 80 μrad to produce a small footprint on the planet to minimize pulse spreading during off-nadir measurements. A sapphire window was used on top of the laser beam expander to reduce thermal distortion to the collimating lens. There were four receiver telescopes with a combined aperture size equivalent to

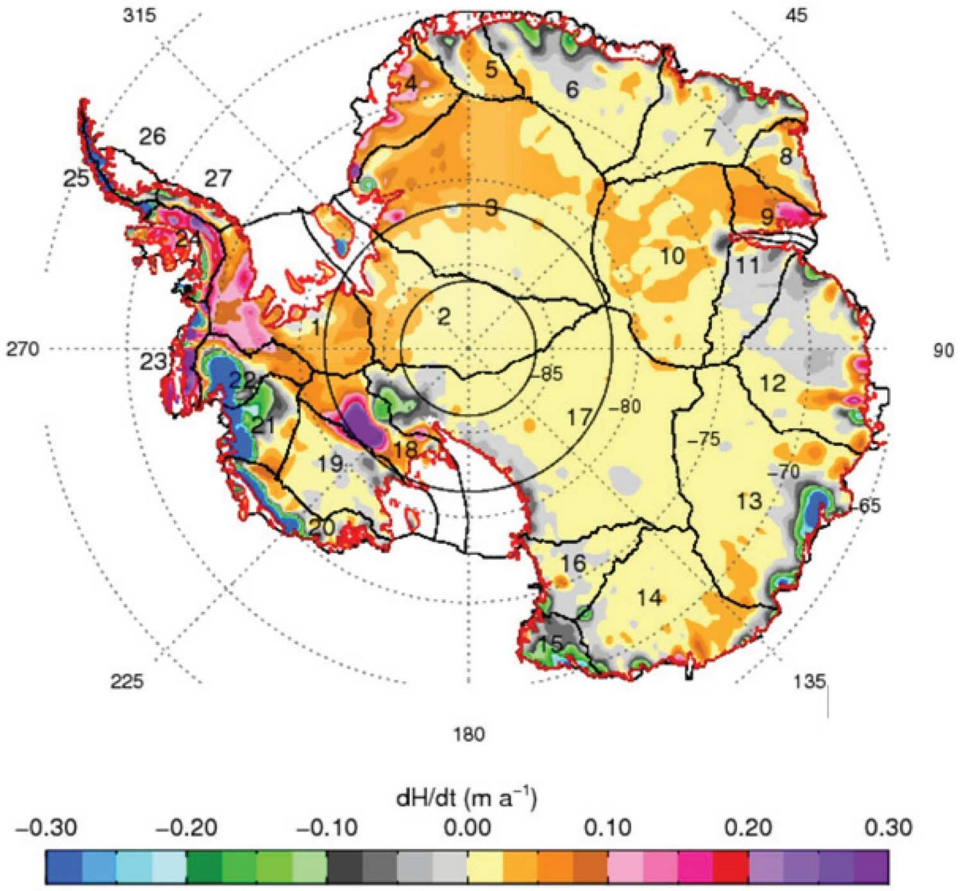

Fig. 9. Annual change in the elevation of the Antarctic icesheet based on GLAS measurements.

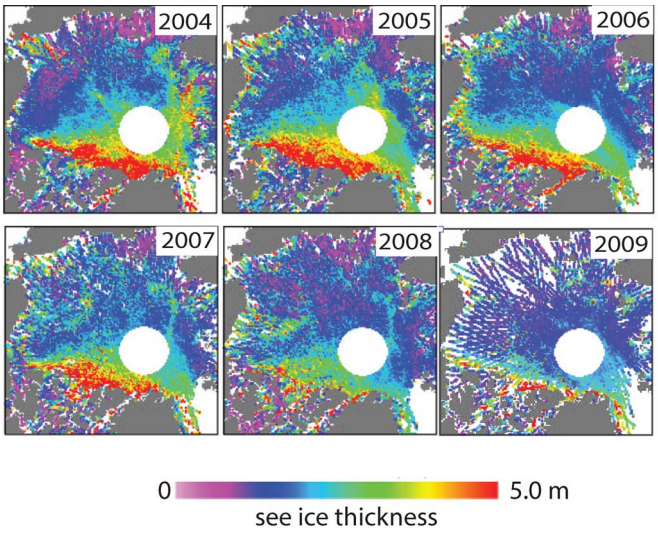

Fig. 10. Arctic winter sea-ice thickness measured by GLAS from 2004 to 2009. The high range precision, 2.0 cm standard deviation, enabled GLAS to identify open water leads and precisely determine the sea-ice thickness and monitor its seasonal changes [39].

that of a single 25-cm diameter telescope [46]. Four smaller refractive telescopes were chosen instead of a large reflective one because it was too difficult for a single reflective telescope to maintain focus under intense heat from sunlit side of Mercury. Sapphire lenses were selected because of their ability to withstand rapid thermal transients and resistance to darkening by space radiation. The signals from each telescope were transmitted and combined onto a single detector via optical fibers [46]. The receiver FOV was designed to be as narrow as possible to minimize background light from the sunlit Mercury while maintaining bore-sight alighment under extreme thermal environment.

The MLA receiver used the same silicon APD detector as in GLAS, followed by three low-pass matched filters, similar to MOLA. The MLA receiver uses a two-threshold and multiple pulse detection technique. The upper threshold is the same as in MOLA, detecting and registering the first pulse above the threshold after the range gate opens. The lower threshold is set at a fraction of the upper threshold. Up to 10 pulses from the low-threshold comparator output within the range gate are recorded for each transmitted laser pulse. Onboard processing software determines the target echo arrival times from the upper threshold crossing whenever it occurs and finds the matching lower threshold crossings to give a four-point sampling of the received pulse. When there is no upper threshold crossings, the software determines the ground return from the low-threshold comparator output based on a histogram of received data from a series of laser shots and identifies those points that form a continuous surface profile. For relatively strong signals, such as at

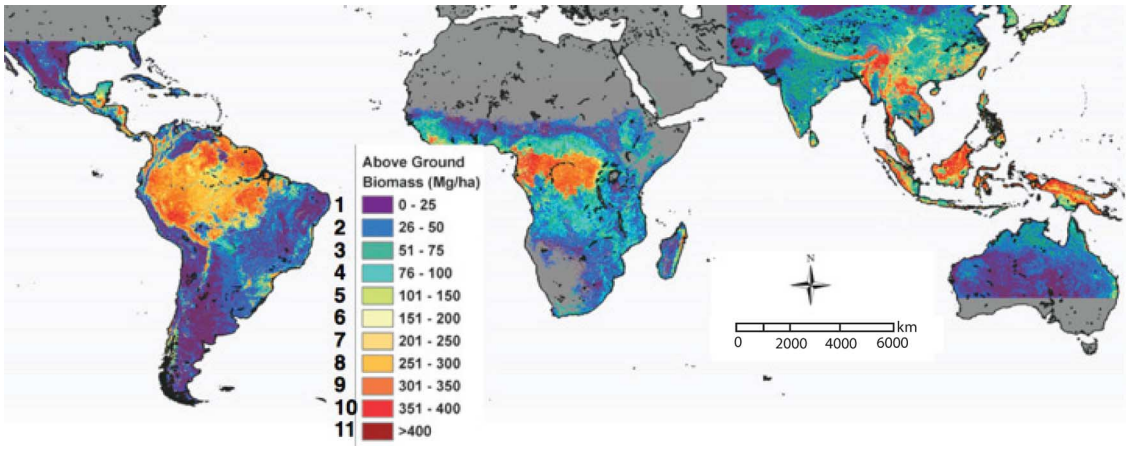

Fig. 11. A partial vegetation map of Earth from a combination of *in situ* survey, GLAS measurements, and optical and microwave imagery [40].

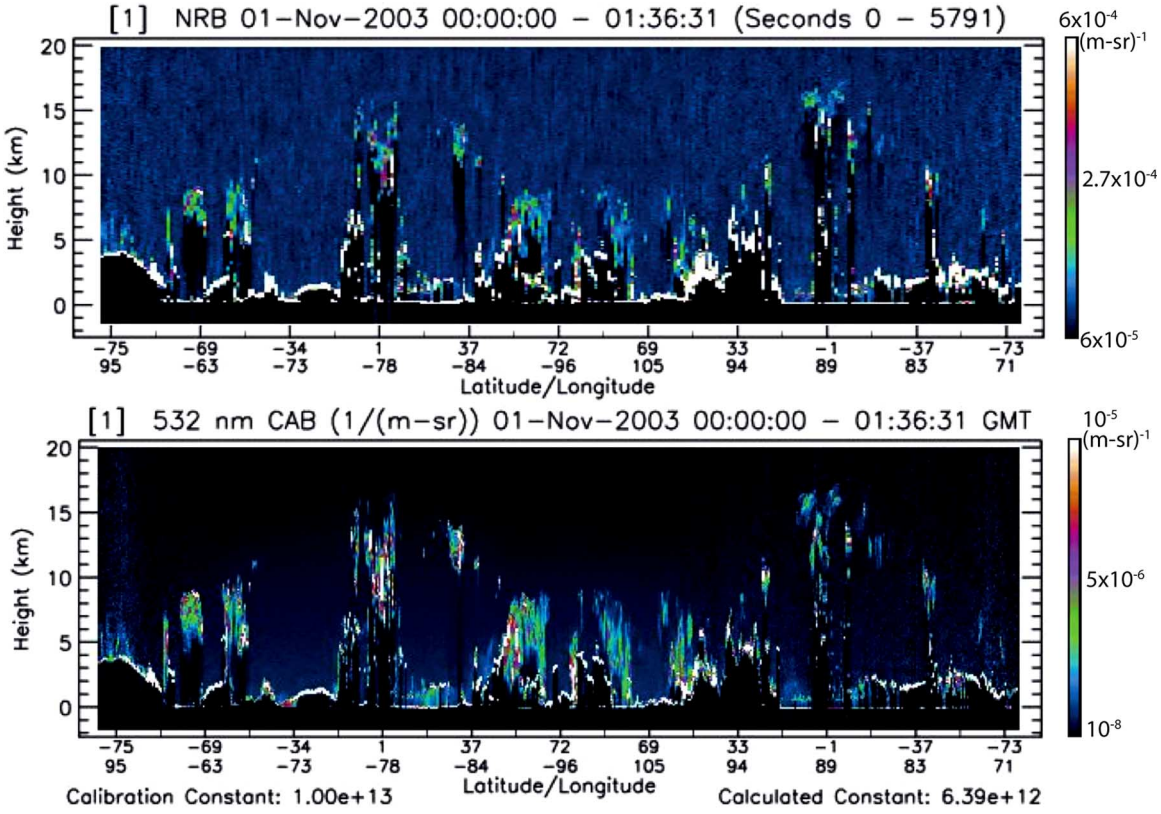

Fig. 12. Sample GLAS atmosphere backscattering measurement at 1064-nm and 532-nm wavelength. The 1064-nm channel was able to detect clouds and aerosols with a cross section as low as 10^{-6}/m-sr. The 532-nm channel was about 10 times more sensitive than the 1064-nm channel and can detect aerosol with a cross section as low as 10^{-7}/m-sr [42].

closer ranges, these four samples of the received pulse waveform at the two thresholds can be used to estimate the received pulse energy and give a measure of surface reflectance to the laser light. The MLA range gate is set according to the predicted range in real time from the spacecraft along the line-of-sight of the laser beam to Mercury surface. The range gate width is set according to the predicted range rate and the surface topography, similar to MOLA and GLAS.

MESSENGER was launched on August 3, 2004, and after a six-and-half-year journey through the inner solar system and six planetary flybys (including three by Mercury), entered Mercury orbit in March 2011. MLA successfully measured the topography profiles over equatorial regions of Mercury during the first two flybys in 2008 [47]. MLA began collecting science measurements from orbit on 29 March 2011 and is still operating to this date. As of 31 Dec. 2012, MLA has collected roughly 11 million topographic measurements of Mercury out of 19 million laser firings over the course of 7 Mercury years [48]. MLA has produced a topographic map of the northern hemisphere of Mercury during the MESSENGER primary science mission and the first extended science mission, as shown in Fig. 15 [49], [50].

Despite the large thermal transients and constant thermal cycling, the MLA optics remain aligned and in focus. The maximum ranging distance achieved by MLA is 1600 km

TABLE III
ICESAT/GLAS OPERATING HISTORY. THERE WERE THREE LASERS, LASER 1 (RED), LASER 2 (LIGHT GREEN), AND LASER 3 (GREEN), EACH WAS OPERATED FOR SEVERAL 30–60 DAY SCIENCE CAMPAIGN PERIOD, FOR EXAMPLE, L2A INDICATES LASER 2, CAMPAIGN PERIOD A [43]

	Jan	Feb	Mar	Apr	May	Jun	Jul	Aug	Sep	Oct	Nov	Dec
2003	Launch		L1							L2a		
2004		L2b				L2c				L3a		
2005		L3b				L3c				L3d		
2006		L3e				L3f				L3g		
2007			L3h							L3i		
2008			L3j							L3k	L2d	
2009			L2e							L2f		
2010		End of Mission Tests						Re-entry				

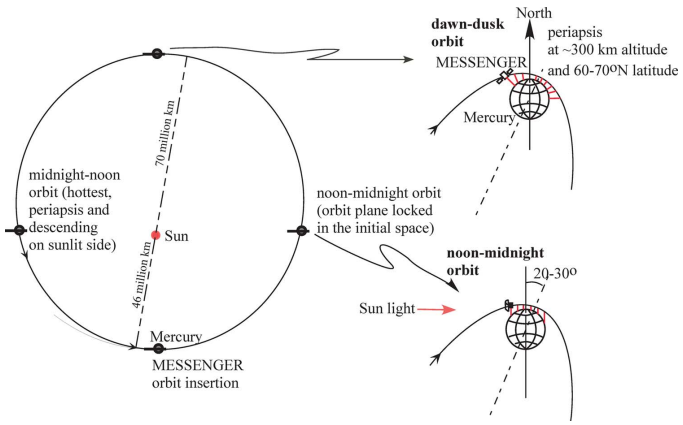

Fig. 13. MERCURY and MESSENGER orbit, and MLA measurement conditions [44].

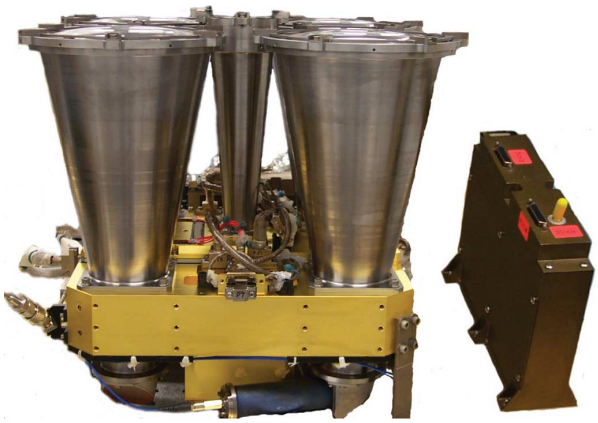

Fig. 14. Photograph of MLA at GSFC prior to delivery to MESSENGER [9]. The diameter of the four received telescopes is 14 cm.

in the nadir direction and 600 km at a 60° slant angle [48]. MLA measurements have extended to the equator and, in many places, beyond the equator during the primary science mission period, as shown in Fig. 15, despite MESSENGER's eccentric orbit and high northern periapsis. A map of surface slopes has been generated from topographic measurements that distinguish volcanic smooth plains from older cratered terrain [50]. MLA measures surface reflectance, including areas in permanent shadow in Mercury's north polar region [51]. MLA measurements of Mercury are continuing during MESSENGER's extended mission [52].

V. LOLA ON THE LRO MISSION

The Lunar Orbiter Laser Altimeter (LOLA) is one of six instruments on the Lunar Reconnaissance Orbiter (LRO) and was developed during 2005–2008. The primary objectives for LOLA are to provide a geodetic map of lunar topography at better than 25-m spatial resolution in the polar region, identify the permanently shadowed regions, and assist in the understanding of volatiles in permanently-shadowed craters [15], [17]. The approach for LOLA took advantage of its relatively low (∼50 km) altitude orbit, which significantly reduced the required laser pulse energy and allowed the use of a single-stage laser splitting into multiple beams. LOLA has two single-stage passively Q-switched lasers, one prime and one spare. The laser design was adapted from the laser oscillator stage of the GLAS laser oscillator with about 3-mJ output pulse energy and a 28-Hz pulse rate [53]. A diffractive optical element (DOE) [54], [55] splits the laser emission into five separate beams so that each laser pulse produces five laser spots on the lunar surface separated by 25 meters in a cross pattern as shown in Fig. 16. LOLA has five independent receiver channels, one for each laser spot on ground. This arrangement allows a two dimensional measurement from a single laser pulse and determining the surface height, slope, and orientation at the same time. Fig. 16 shows the laser beam footprint pattern and the receiver FOV on the lunar surface from a nominal 50 km altitude orbit [15].

Like MLA, LOLA operates in a highly variable thermal environment. Since the moon rotates slowly and does not have an atmosphere, the surface temperature difference between the sunlit side to the dark side is as high as 250 K. As a result, LOLA experiences a large-swing thermal cycling every orbit (two hours)

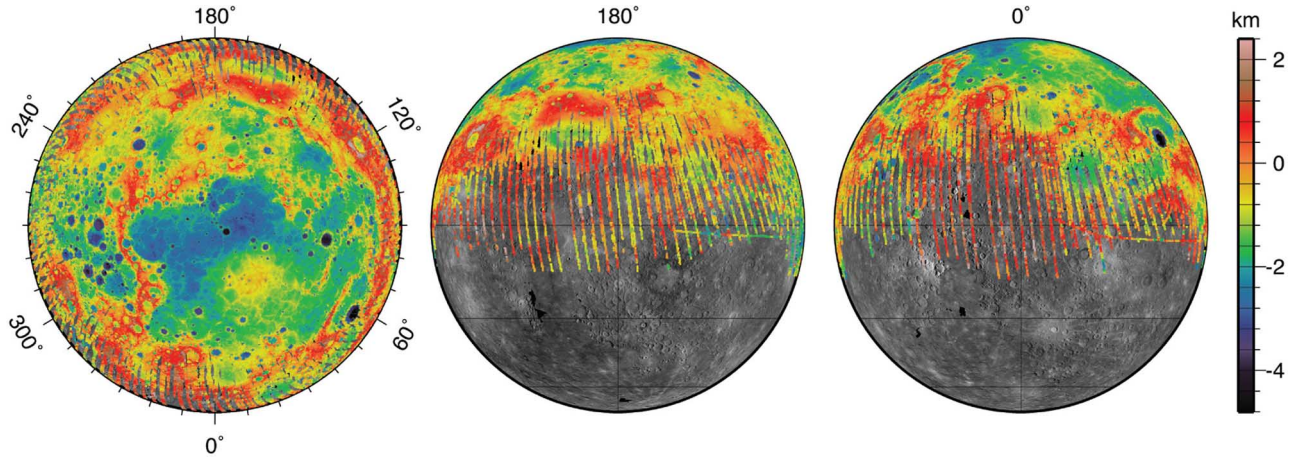

Fig. 15. MLA measurement coverage up to 23 February 2013 overlaid on a monochromatic image mosaic of Mercury from the camera on MESSENGER. View from North Pole (left), at 180° longitude (center), and 0° longitude (right).

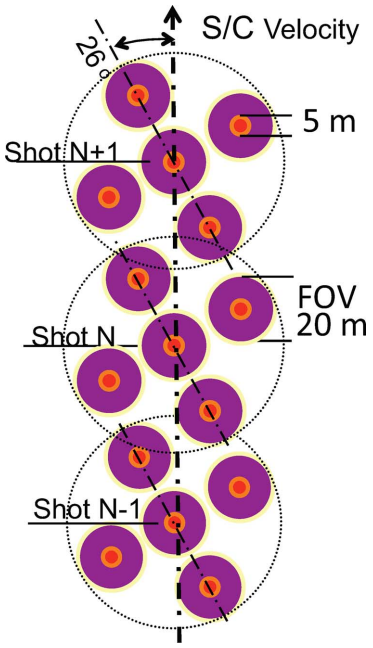

Fig. 16. LOLA laser footprint and receiver field of view [15].

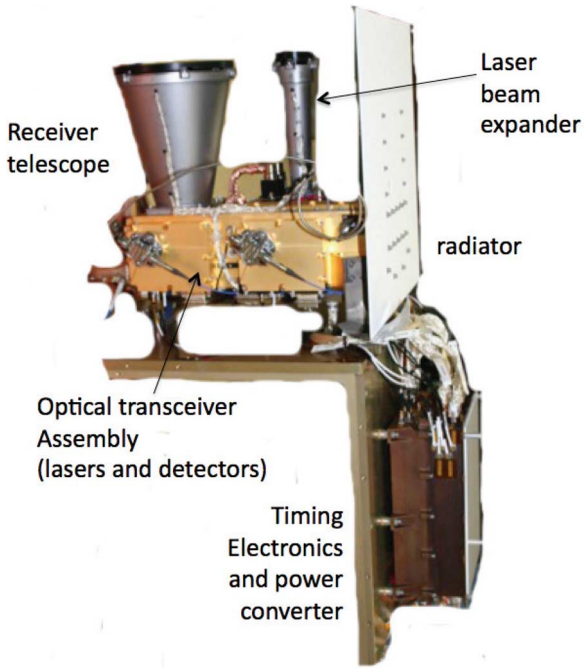

Fig. 17. Photograph of LOLA prior to delivery to LRO [15].

and a thermal shock every time it crosses the terminator. Fig. 17 shows a photograph of LOLA.

LRO also carries a novel laser ranging (LR) receiver that allows it to detect 532-nm laser pulses from satellite laser ranging (SLR) stations on the Earth. The LR receiver consists of a small telescope that is mounted on and co-boresighted with the LRO high gain antenna. The LR signal is relayed via optical fibers to LOLA for time-tagging [16]. With atomic clocks at the ground stations and a highly stable quartz USO on the spacecraft, this allows one-way laser ranging measurements of the relative distance of the LRO spacecraft from Earth. This helps to better determine the LRO orbital position.

LRO was launched in June 2009 and since then LOLA has collected over 6 billion measurements of lunar topography to this date [56], [57]. LOLA has supported one-way laser ranging operation from ten SLR stations from four continents. To date, the LOLA along-track measurement resolution (north-south) is 20–30 m and the ground track spacing in the east-west direction is 300 m at equator (0.01°). Simultaneous multi-beam measurements provided by LOLA give surface slope and orientation between laser spots on the surface. The surface slope and roughness within the laser footprints can be derived from the received pulse width. The multi-beam configuration also helps constrain the location of crossover points along the ground tracks. This significantly improves orbit determination and thereby the footprint elevations and the lunar gravity field.

LOLA also measures the lunar surface reflection at zero phase angle, which gives the so-called normal albedo and reveals more features of the lunar surface [58]. LOLA measures the shape and reflectance of permanently-shadowed craters that have never been imaged by cameras [59]. Fig. 18 shows four types of lunar data provided by LOLA, which are available from the Planetary Data System (PDS). LRO is currently in its extended science

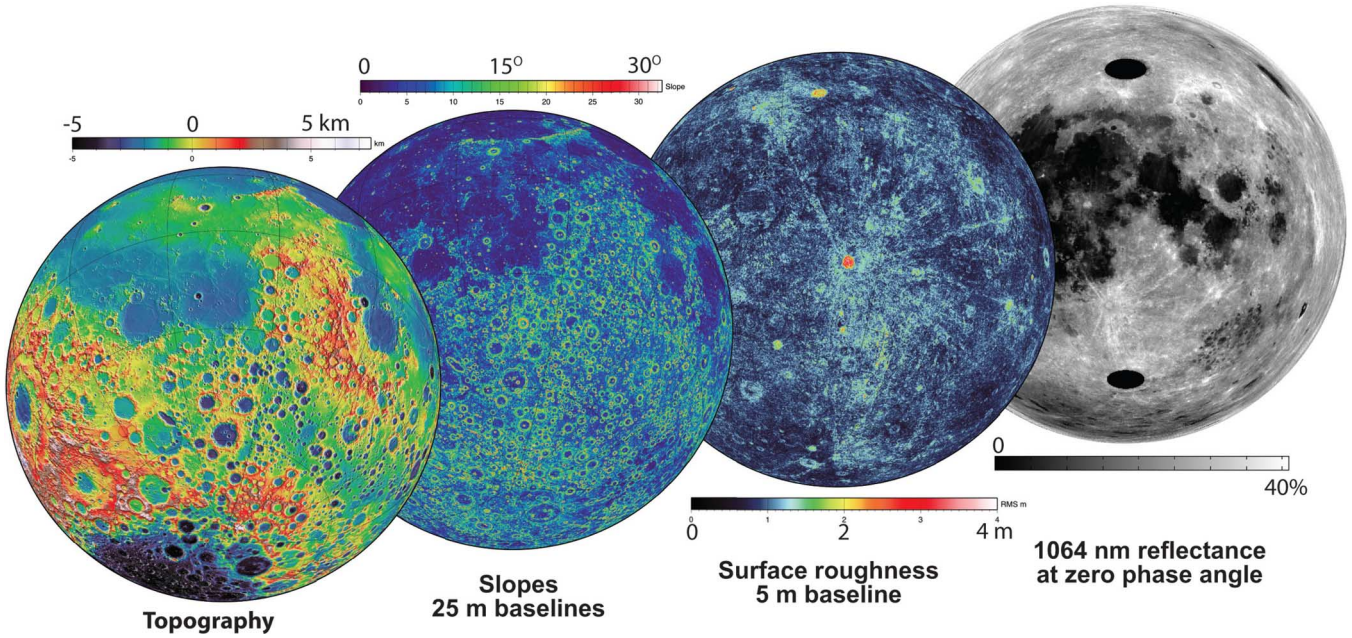

Fig. 18. The four types of lunar data that LOLA provides to the Planetary Data System (PDS).

mission, in a low-maintenance elliptical orbit, and LOLA measurements are expected to continue in the coming years.

VI. In Space Calibrations

In-space calibration experiments have been carried out for each instrument described above by having the corresponding spacecraft point the lidar toward Earth, and scan the instrument pointing across the ground station at NASA GSFC. Laser pulses were transmitted simultaneously between the lidar in space and ground station at GSFC. The laser pulse arrival times and spacecraft pointing data were used to estimate the laser pointing angle with respect to the spacecraft coordinate system, the receiver boresight, and co-alignment with the camera. The results were also used to verify spacecraft and instrument timing. In addition, these tests served as technology demonstrations for freespace laser communications and long distance laser ranging and tracking.

In May 2005, an MLA in-space calibration was performed by scanning its laser beam across the SLR station at NASA GSFC in a two-way laser ranging and asynchronous laser transponder configuration over 24 million km [60], [61]. An Earth-to-MOLA laser transmission test was successfully conducted at a distance of 81 million km in September 2005 [62]. A series of two-way laser ranging tests between LOLA and the SLR station at NASA GSFC were conducted in September 2009. GLAS/ICESat was pointed to NASA GSFC routinely to compare the atmosphere measurement with a ground-based lidar measurement. During the orbital overpass in November 2006, GLAS laser pulse waveforms were directly captured using a GLAS flight-spare detector and oscilloscope. GLAS was also pointed at Venus in March 2010 near the end of the ICESat mission and detected starshine signal from 1064-nm and 532-nm channel outputs, which confirmed a pointing bias of the GLAS laser beam with respect to the spacecraft coordinate system. Recently, a free-space laser communication experiment was conducted from the SLR station at NASA GSFC to LRO via the LR receiver, successfully demonstrating simultaneous laser ranging and lunar laser communication over 380,000 km [63]. More details of these experiments will be described in the future.

VII. Summary

NASA Goddard Space Flight Center (GSFC) has successfully developed five space-borne lidar on orbital missions. They were the Mars Orbiter Laser Altimeter (MOLA) on the Mars Observer mission in 1992 and Mars Global Surveyor (MGS) mission in 1996, respectively, the Geoscience Laser Altimeter System (GLAS) on the Ice, Cloud, and land Elevation Satellite (ICESat) mission in 2003, the Mercury Laser Altimeter (MLA) on the MErcury Surface, Space ENvironment, Geochemistry, and Ranging (MESSENGER) mission in 2004, and the Lunar Orbital Laser Altimeter (LOLA) on the Lunar Reconnaissance Orbiter (LRO) mission in 2009. All of them used diode-pumped Q-switched Nd:YAG lasers with 5–8 nsec wide pulses at 8–40 Hz pulse rates and direct detection receivers with silicon avalanche photodiodes (APD) detectors.

MOLA was the first space lidar to map a planet. GLAS was the first orbiting lidar to accurately map both icesheet and land on Earth. MLA was a miniaturized version of MOLA with extended range and ability to withstand a much more severe thermal environment. LOLA was similar to MLA but with five beams from a single laser. These laser altimeters were designed not only to measure range but also surface slopes, roughness, and reflectance of laser and sun light. They have provided detailed topographic maps of Mars, Earth, Moon, and the northern hemisphere of Mercury, and dramatically improved our understanding of these planets. Two of these instruments, MLA and LOLA, are still operating to this date.

NASA GSFC is continuing to develop space lidar with advanced capabilities for new applications. The major areas of

developments are in new types of applications and multi-beam measurements. These require lasers with higher power efficiency and longer lifetimes, photon counting detectors at visible and infrared wavelengths, and improved signal processing. A team at GSFC is currently building the Advanced Topographic Laser Altimeter System (ATLAS) for the ICESat-2 mission [64]. ATLAS is a six-beam laser altimeter with multi-kHz pulse rate lasers and photon-counting receivers, which, compared to GLAS, will improve spatial coverage and provide cross track slope measurements. Several new lidar approaches are also being developed under the research-and-development programs from NASA's Earth Science Technology Office (ESTO). These include the laser sounder approach to measure CO_2 and O_2 column abundance for the Active Sensing of CO_2 Emission over Days, Nights, and Seasons (ASCENDS) mission, and the wide swath multi-beam swath-mapping lidar for the LIdar Surface Topography (LIST) mission.

ACKNOWLEDGMENT

The authors thank the NASA GSFC management for their strong and sustained support in developing lidar technologies and space lidar instruments. They thank S. Saatchi for providing the map of tropical canopy and R. Kwok for permission to use the images of sea-ice thickness. They thank D. Yi for providing the GLAS measurement data from Lake Vostok. They thank J. DiMarzio for providing the Antarctic and Greenland elevation map from GLAS measurements. They thank E. Mazarico and M. Torrence for providing the global maps of the moon from the LOLA data. Finally, they thank the instrument teams at NASA GSFC for the design, fabrication and tests of these space lidar.

REFERENCES

[1] M. T. Zuber *et al.*, "Mars Observer Laser Altimeter investigation," *J. Geophys. Res.*, vol. 97, no. E5, pp. 7781–7797, May 1992.

[2] A. A. Albee, F. D. Palluconi, and R. E. Arvidson, "Mars Global Surveyor mission: Overview and status," *Science*, vol. 279, no. 5357, pp. 1671–1672, 1998.

[3] M. T. Zuber *et al.*, "Observation of the north polar of Mars from the Mars Orbiter Laser Altimeter," *Science*, vol. 282, no. 5396, pp. 2053–2060, Dec. 11, 1998.

[4] D. E. Smith *et al.*, "Mars Orbiter Laser Altimeter (MOLA): Experiment summary after the first year of global mapping of Mars," *J. Geophys. Res.*, vol. 106, no. E10, pp. 23689–23722, Oct. 2001.

[5] H. J. Zwally *et al.*, "ICESat's laser measurements of polar ice, atmosphere, ocean, and land," *J. Geodyn.*, vol. 34, pp. 405–445, 2002.

[6] H. J. Zwally and B. E. Schutz, "Results from Ice, Cloud, and Land Elevation Satellite (ICESat) mission," *Geophys. Res. Lett.*, vol. 32, no. 21–23, 2005, AGU, Washington DC, Reprinted from.

[7] B. E. Schutz *et al.*, "Overview of the ICESat mission," *Geophys. Res. Lett.*, vol. 32, p. L21S01, 2005.

[8] J. B. Abshire *et al.*, "Geoscience Laser Altimeter System (GLAS) on the ICESat mission: On-orbit measurement performance," *Geophys. Res. Lett.*, vol. 32, p. L21S02, 2005.

[9] X. Wang *et al.*, "Earth science applications of ICESat/GLAS: A review," *Int. J. Remote Sens.*, vol. 32, no. 23, pp. 8837–8864, Dec. 2011.

[10] J. F. Cavanaugh *et al.*, "The Mercury Laser Altimeter instrument for the MESSENGER mission," *Space Sci. Rev.*, vol. 131, no. 1–4, pp. 451–479, Aug. 2007.

[11] D. L. Domingue and C. T. Russell, Eds., *The MESSENGER Mission to Mercury*. New York, NY, USA: Springer, 2007.

[12] S. C. Solomon, R. L. McNutt, Jr., R. E. Gold, and D. L. Domingue, "MESSENGER mission overview," *Space Sci. Rev.*, vol. 131, pp. 3–39, 2007.

[13] S. C. Solomon *et al.*, "Return to Mercury: A global perspective on MESSENGER's first Mercury flyby," *Science*, vol. 321, 2008.

[14] X. Sun *et al.*, "Mapping the topography of Mercury with MESSENGER laser altimetry," *SPIE Newsroom*, Oct. 26, 2012, dio. 10.1117/2.1201210.004489.

[15] D. E. Smith *et al.*, "The Lunar Orbiter Laser Altimeter investigation on the Lunar Reconnaissance Orbiter mission," *Space Sci. Rev.*, vol. 150, no. 1–4, pp. 209–241, Jan. 2010.

[16] M. T. Zuber *et al.*, "The Lunar Reconnaissance Orbiter Laser Ranging investigation," *Space Sci. Rev.*, vol. 150, no. 1–4, pp. 63–80, Jan. 2010.

[17] *Lunar Reconnaissance Orbiter Mission*, R. R. Vondrak, J. W. Keller, and C. T. Russell, Eds. New York, NY, USA: Springer, 2010.

[18] R. S. Afzal, "The Mars Observer Laser Altimeter: Laser transmitter," *Appl. Opt.*, vol. 33, no. 15, pp. 3184–3188, 1994.

[19] S. Nozette *et al.*, "The Clementine mission to the moon: Scientific overview," *Science*, vol. 266, pp. 1835–1839, 1994.

[20] M. T. Zuber *et al.*, "The shape and internal structure of the moon from the Clementine mission," *Science*, vol. 266, pp. 1839–1843.

[21] *The Near Earth Asteroid Rendezvous Mission*, C. T. Russell, Ed. Dordrecht, The Netherlands: Kluwer, 1997.

[22] T. D. Cole, "The Near-Earth Asteroid Rendezvous laser altimeter," *Space Sci. Rev.*, vol. 82, pp. 217–253, 1997.

[23] J. B. Abshire *et al.*, "Mars Orbiter Laser Altimeter: Receiver model and performance analysis," *Appl. Opt.*, vol. 39, no. 15, pp. 2449–2460, May 2000.

[24] J. L. Bufton, "Laser altimetry measurements from aircraft and spacecraft," *Proc. IEEE*, vol. 77, no. 3, pp. 463–477, 1989.

[25] L. Ramos-Izquierdo, J. L. Bufton, and P. Hayes, "Optical system design and integration of the Mars Observer Laser Altimeter," *Appl. Opt.*, vol. 33, no. 3, pp. 307–322, 1994.

[26] F. Laforce, "Optical receiver using silicon APD for space applications," in *Proc. SPIE 7330*, 2009, pp. 73300R-1–73300R-12.

[27] G. A. Neumann *et al.*, "Mars Orbiter Laser Altimeter pulsewidth measurements and footprint-scale roughness," *Geophys. Res. Lett.*, vol. 30, no. 1561, pp. 15-1–15-4, 2003.

[28] G. A. Neumann *et al.*, "Two Mars years of clouds detected by the Mars Orbiter Laser Altimeter," *J. Geophys. Res.*, vol. 108, no. E4, pp. 4-1–4-10, 2003.

[29] X. Sun *et al.*, "Mars 1064 nm spectral radiance measurements determined from the receiver noise response of the Mars Orbiter Laser Altimeter," *Appl. Opt.*, vol. 45, no. 17, pp. 2960–3971, 2006.

[30] M. T. Zuber and D. E. Smith, "Observations of the seasonal polar icecaps of Mars at 1064 nm," in *Proc. 3rd Int. Conf. Mars Polar Sci.*, AB, Canada, Oct. 13–17, 2003, Paper 8032.

[31] J. Garvin *et al.*, "Observations of the Earth's topography from the Shuttle Laser Altimeter (SLA): Laser-pulse echo-recovery measurements of terrestrial surfaces," *Phys. Chem. Earth*, vol. 23, no. 9–10, pp. 1053–1068, 1998.

[32] R. S. Afzal *et al.*, "The Geoscience Laser Altimeter System (GLAS) laser transmitter," *IEEE J. Sel. Topics Quantum Electron.*, vol. 13, no. 3, pp. 511–536, May/Jun. 2007.

[33] J. M. Sirota *et al.*, "The transmitter pointing determination in the Geoscience Laser Altimeter System," *Geophys. Res. Lett.*, vol. 32, p. L21S11, 2005.

[34] M. A. Krainak *et al.*, "Comparison of linear-mode avalanche photodiode lidar receivers for use at one micron wavelength," in *SPIE 7681*, 2010, paper 7681-34.

[35] H. J. Zwally *et al., GLAS/ICESat L2 Antarctic and Greenland Ice Sheet Altimetry Data V001*. Boulder, CO: Digital media, 2003 [Online]. Available: http://nsidc.org/data/docs/daac/glas_icesat_l1_l2_global_altimetry.gd.html, National Snow and Ice Data Center (NSIDC).

[36] X. Sun *et al.*, "Cloud and aerosol lidar channel design and performance of the Geoscience Laser Altimeter System on the ICESat mission," in *Proc. CLEO*, 2004, vol. 2, Paper CTh16.

[37] X. Sun *et al.*, "Space-qualified silicon avalanche-photodiode single-photon-counting modules," *J. Modern Opt.*, vol. 51, no. 9–10, pp. 1333–1350, Jun.–July 2004.

[38] H. Fricker *et al.*, "Assessment of ICESat performance at the salar de Uyuni, Bolivia," *Geophys. Res. Lett.*, vol. 32, p. L21S06, 2005, doi:10.1029/2005GL023423.

[39] R. Kwok *et al.*, "Thinning and volume loss of the Arctic ocean sea ice cover: 2003–2008," *J. Geophys. Res.*, vol. 114, 2009, doi:10.1029/2009JC005312.

[40] S. S. Saatchi *et al.*, "Benchmark map of forest carbon stocks in tropical regions across three continents," in *Proc. Nat. Acad. Sci.*, Jun. 2011, vol. 108, no. 24, pp. 9899–9904.

[41] D. J. Harding *et al.*, "ICESat waveform measurements of within-footprint topographic relief and vegetation vertical structure," *Geophys. Res. Lett.*, vol. 32, 2005, doi:10.1029/2005GL023471.
[42] J. D. Spinhirne *et al.*, "Cloud and aerosol measurements from GLAS: Overview and initial results," *Geophys. Res. Lett.*, vol. 32, 2005, doi: 10.1029/2005GL023507.
[43] X. Sun *et al.*, "Performance assessment of the Geoscience Laser Altimeter System (GLAS) through the end of seven-year mission in space," in *Proc. CLEO*, 2011, Paper ATuA2.
[44] X. Sun *et al.*, "Mercury Laser Altimeter—Instrument design, testing, and performance verification," in *Proc. ILRC*, Matera, Italy, Jul. 12–16, 2004, pp. 961–964.
[45] D. J. Krebs *et al.*, "Compact, passively *Q*-switched Nd:YAG laser for the MESSENGER mission to Mercury," *Appl. Opt.*, vol. 44, no. 9, pp. 1715–1718, Mar. 2005.
[46] L. Ramos-Izquierdo *et al.*, "Optical system design and integration of the Mercury Laser Altimeter," *Appl. Opt.*, vol. 44, no. 9, pp. 1748–1760, Mar. 2005.
[47] M. T. Zuber *et al.*, "Laser altimeter observations from MESSENGER's first Mercury flyby," *Science*, vol. 321, no. 5885, pp. 77–79, Jul. 2008.
[48] X. Sun *et al.*, "Mapping the topography of Mercury with MESSENGER laser altimetry," in *Proc. SPIE Newsroom*, Oct. 26, 2012, dio. 10.1117/2.1201210.004489.
[49] D. E. Smith *et al.*, "Gravity field and internal structure of Mercury from MESSENGER," *Science*, vol. 336, no. 6078, pp. 214–217, Apr. 2012.
[50] M. T. Zuber *et al.*, "Topography of the northern hemisphere of Mercury from MESSENGER laser altimetry," *Science*, vol. 336, no. 6078, pp. 217–220, Apr. 2012.
[51] G. A. Neumann *et al.*, "Bright and dark polar deposits on Mercury: Evidence for surface volatiles," *Science*, vol. 339, pp. 296–300, 2013.
[52] [Online]. Available: http://messenger.jhuapl.edu
[53] A. Y. Yu *et al.*, "The Lunar Orbiter Laser Altimeter (LOLA) laser transmitter," *SPIE*, vol. 6871, p. 68710D, 2008.
[54] L. Ramos-Izquierdo *et al.*, "Optical system design and integration of the Lunar Orbiter Laser Altimeter," *Appl. Opt.*, vol. 48, pp. 3035–3049, 2009.
[55] J. G. Smith *et al.*, "Diffractive optics for moon topography mapping," in *Proc. SPIE*, 2006, vol. 6223, p. 622304.
[56] D. E. Smith *et al.*, "Initial observations from the Lunar Orbiter Laser Altimeter (LOLA)," *Geophys. Res. Lett.*, vol. 37, p. L18204, 2010.
[57] D. E. Smith *et al.*, "Space lidar measurements of Mars the moon and Mercury," in *Proc. IGARSS*, Munich, Germany, Jul. 22–27, 2012, Paper TH4.11.4.
[58] M. A. Riner *et al.*, "Exploring the lunar poles—The normal albedo of the moon from LOLA," in *Proc. American Geophysical Union, Fall Meeting 2011*, abstract #P13D-1707.
[59] M. T. Zuber *et al.*, "Constraints on the volatile distribution within Shackleton crater at the lunar south pole," *Nature*, vol. 486, pp. 378–381, 2012.
[60] M. T. Zuber, "Seconds of data, years of trying," *Photon. Spectra*, pp. 56–62, May 2006.
[61] D. E. Smith *et al.*, "Two-way laser link over interplanetary distance," *Science*, vol. 311, no. 5757, p. 53, Jan. 2006.
[62] J. B. Abshire *et al.*, "Laser pulses from earth detected at Mars," in *Proc. CLEO/IQEC*, May 25, 2007, Paper CThT6.
[63] X. Sun *et al.*, "Free space laser communication experiments from earth to the lunar reconnaissance orbiter in lunar orbit," *Opt. Exp.*, vol. 21, no. 2, pp. 1865–1871, Jan. 2013.
[64] W. Abdalati *et al.*, "The ICESat-2 laser altimeter mission," *Proc. IEEE*, vol. 98, no. 5, pp. 735–751, May 2010.

Xiaoli Sun (S'88–M'90) received the B.S. degree from Taiyuan Institute of Technology, Taiyuan, China, in 1982, and the Ph.D. degree in electrical engineering from the Johns Hopkins University, Baltimore, MD, USA, in 1989.

He is now a Senior Scientist at the Solar System Exploration Division at NASA's Goddard Space Flight Center, Greenbelt, MD, USA. He was the Lead Engineer in photodetector development and receiver performance analysis for the Mars Orbiter Laser Altimeter on the Mars Global Surveyor Mission and the Geoscience Laser Altimeter System on the ICESat Mission. He was the instrument scientist for the Mercury Laser Altimeter on the MESSENGER mission and the Lunar Orbiter Laser Altimeter and the one-way laser ranging on the Lunar Reconnaissance Orbiter (LRO) mission. He led the first two-way laser ranging experiment between the MESSENGER spacecraft and Earth over 24 million km in 2005, and the first lunar laser communication experiments from Earth to LRO in 2012. He is the lead of the infrared detector development and receiver modeling for the CO_2 lidar for the ASCENDS mission.

James B. Abshire (S'73–M'81–SM'85) received the B.S. degree from the University of Tennessee, Knoxville, TN, USA, in 1974, and the Ph.D. degree from the University of Maryland, College Park, MD, USA, in 1982, both in electrical engineering.

He is presently the Senior Scientist for Laser Sensing for the Solar System Exploration Division at NASA's Goddard Space Flight Center, Greenbelt, MD, USA. He has helped lead the development of space lidar at Goddard, and was Instrument Scientist on the Mars Orbiter Laser Altimeter on the Mars Global Surveyor Mission and the Geoscience Laser Altimeter System on the ICESat Mission. He currently is leading Goddard's work in remotely measuring atmospheric CO_2 with lidar and serves on the formulation teams for the NASA ASCENDS mission and the French/German MERLIN mission.

Dr. Abshire is a member of the IEEE, Optical Society of America, American Geophysical Union and European Geophysical Union. He is serving co-chair of the lidar working group in the Instrument Future Technology Committee of the IEEE GRSS.

Jan F. McGarry received the B.A. degree in mathematics from Goucher College, Towson, MD, USA, in 1974, and the M.A. degree in applied mathematics from the University of Maryland, College Park, MD, USA, in 1983.

She started working at NASA as a mathematician in 1974 immediately after graduating from college. She has worked in Satellite Laser Ranging and Laser Altimetry throughout her career, developing instrument control software, modeling hardware and developing software simulators, generating mathematical algorithms to optimize system performance, and performing data analysis for ground-based, space-based and airborne systems. She was the science algorithm leads for MOLA, MLA, GLAS and LOLA. She is currently leading the development of NASA's Next Generation Satellite Laser Ranging System, and is also the science algorithm subsystem lead for the ATLAS instrument onboard ICESat-2, a NASA's Earth Science mission scheduled to be launched in 2016.

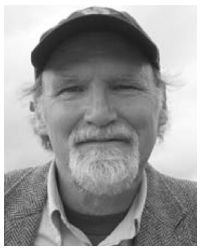

Gregory A. Neumann was born in Washington, D.C., and received the B.A. degree in mathematics from Reed College, Portland, OR, USA, in 1969 and the M.S. and Ph.D. degrees in geological sciences from Brown University, Providence, RI, USA, in 1991 and 1993.

From 1993 to 2005 he was a Research Scientist at The Johns Hopkins University and the Massachusetts Institute of Technology. Since 2005 he has been a geophysicist at the NASA Goddard Space Flight Center, Greenbelt, Maryland. He has led the analysis of laser altimetry from the Clementine, Mars Global Surveyor, NEAR-Shoemaker, MESSENGER, and Lunar Reconnaissance Orbiter missions as well as participating in the Dawn and GRAIL missions. He specializes in the use of laser altimetry, sonar bathymetry, gravity, and magnetics to interpret planetary crustal structure. He has authored and co-authored more than 90 journal articles and has produced graphics from planetary topography for popular magazines and textbooks.

Mr. Neumann has received the 2011 Robert H. Goddard award for Scientific Achievement and numerous other NASA awards. He has been a member of the American Geophysical Union since 1982.

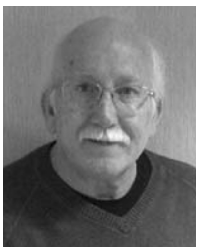

James C. Smith received the B.S.E.E. degree from the University of Maryland, College Park, MD, USA, in May 1978.

He has been with NASA Goddard Space Flight Center, Greenbelt, MD, USA, since 1978. During his tenure at Goddard he has involved in the systems design and development of many airborne remote sensors and space borne laser altimeter systems. He was the system engineer of MOLA on the Mars Observer and MGS missions and MLA on MESSENGER mission. He has authored and co-authored numerous articles for in-house publications and peer review journals on space flight instrument designs including laser altimeters, passive radiometers, bench test systems, control circuit applications and unique application specific design solutions.

Mr. Smith has received numerous Special Achievement and Performance Awards for outstanding contributions, including NASA's Exceptional Service Award for his sustained contributions on GSFC's end-to-end spaceflight laser altimeter instrument developments. Mr. Smith is currently involved with the systems concept design and performance analysis for the next generation atmospheric and BRDF aircraft scanning instrument, a LEO large field-of-view photosynthesis radiometer, and a large swath geosynchronous ocean color coastal sensor.

John F. Cavanaugh received the B.S.E.E. degree from the University of Maryland, College Park, MD, in 1988.

He has worked for NASA since 1983, primarily on laser instruments for remote sensing. He has worked on several space-based laser instruments developed at NASA GSFC, serving as the altimetry electronics lead for the Mars Orbiter Laser Altimeter (MOLA), electrical engineer for the Shuttle Laser Altimeter (SLA), instrument systems engineer for the Mercury Laser Altimeter (MLA) and the Lunar Orbiter Laser Altimeter (LOLA).

David J. Harding received the B.S. and Ph.D. degrees in geological sciences from Cornell University, Ithaca, NY, USA, in 1980 and 1988.

Since 1991, he has been a Research Scientist with the NASA Goddard Space Flight Center, Greenbelt, MD, USA, where he currently works in the Planetary Geodynamics Laboratory, Sciences and Exploration Directorate. He conducts research in the topographic expression of land surface processes and the physical properties of vegetation, snow, ice and water, in particular by developing and utilizing advanced airborne and space-based laser altimeter systems. He is the principal investigator for the airborne Slope Imaging Multi-polarization Photon-Counting Lidar (SIMPL), developed through the NASA Instrument Incubator Program. He has authored or coauthored 45 conference proceedings and peer-reviewed papers.

Dr. Harding was a member of the Ice, Cloud and land Elevation Satellite (ICESat) Science Team and is now a member of the ICESat-2 Science Definition Team. In addition, he represented NASA in the Puget Sound Lidar Consortium (PSLC) that conducted comprehensive lidar mapping in the Puget Sound region and Cascades Range, WA, USA.

H. Jay Zwally received the B.S. in mechanical/aeronautical engineering from Drexel University, Philadelphia, PA, USA, and the Ph.D. degree in physics with a minor in mathematics from the University of Maryland, College Park, MD, USA.

He is Chief Cryospheric Scientist at NASA's Goddard Space Flight Center, Greenbelt, MD, USA, and Project Scientist for the Ice Cloud and Land Elevation Satellite (ICESat). His recent research includes leading comprehensive analysis of the mass balance of the Greenland and Antarctic ice sheets and ice shelves, discovery of the melt-acceleration effect on the flow of the Greenland ice sheet, and the first comprehensive mapping of sea ice freeboard and thickness. He led promotion and development of ICESat and was a key participant in the design and planning for ICESat-2. At NASA since 1974, his early research included radiative modeling of microwave emission from snow, development of concepts for remote measurement of accumulation rates and surface melting, and systematic compilation of satellite passive-microwave data sets that led to discovery of the Weddell Polynya and several sea ice atlases. He also pioneered the use of ocean radar altimeters for mapping ice sheet topography and studies of mass balance. Prior to his work at NASA, he was Program Manager for Glaciology and Remote Sensing in the NSF's Division of Polar Programs, where he managed the initiation of the interdisciplinary Ross Ice Shelf Project, the Greenland Ice Sheet Project, improved airborne radar mapping of ice sheet thickness, and planning for West Antarctic ice sheet projects. He has over 150 referred publications in glaciology, polar research, climate science, and physics.

David E. Smith received the B.Sc. degree in 1958 from University of Durham, Durham, U.K., and the Ph.D. degree in 1962 from University of London, London, U.K.

He is the Principal Investigators for the Mars Orbiter Laser Altimeter (MOLA) on the Mars Observer mission and Mars Global Surveyor mission; the Mercury Laser Altimeter (MLA) on the MESSENGER Mission, and the Lunar Orbiter Laser Altimeter (LOLA) on the Lunar Reconnaissance Orbiter (LRO) mission. He is the Deputy Principal Investigator for the Gravity Recovery and Interior Laboratory (GRAIL) Discovery Mission operating in lunar orbit, and is also a Co- Investigator on the Dawn Discovery Mission to Vesta and Ceres, and a member of the Mars Reconnaissance Orbit (MRO) Mission gravity team. He was also the Principal Investigator for laser altimeter on the Clementine mission to the moon with lead responsibilities for gravity and topography, and a member of the Near Earth Asteroid & Rendezvous science team for topography of the asteroid 433 Eros. Prior to MIT, he was on the staff of the Goddard Space Flight Center where he was the Chief of the Laboratory for Terrestrial Physics and subsequently the Deputy Director for Planetary Science in the Solar System and Exploration Division. He was also the Project Scientist for the LAGEOS-1 spacecraft and for the NASA Crustal Dynamics Project for the measurement of plate kinematics.

Maria T. Zuber received the B.A. degree from the University of Pennsylvania, Philadelphia, PA, USA, and the M.Sc. and Ph.D. degrees from Brown University, Providence, RI, USA.

She is the E. A. Griswold Professor of Geophysics at the Massachusetts Institute of Technology, Cambridge, MA, USA, and currently serves as Principal Investigator of NASA's Gravity Recovery and Interior Laboratory (GRAIL) Mission. She has been involved in more than half a dozen NASA planetary missions aimed at mapping the Moon, Mars, Mercury and several asteroids.

Prof. Zuber has won numerous awards including the MIT James R. Killian Jr. Faculty Achievement Award, the American Geophysical Union Harry H. Hess Medal, NASA's Outstanding Public Leadership Medal, Group Achievement Award for the GRAIL Science Team and Outstanding Scientific Achievement Medal, as well as the Geological Society of America G. K. Gilbert Award and the American Astronautical Society/Planetary Society Carl Sagan Memorial Award. She is a member of the National Academy of Sciences and American Philosophical Society, and is a fellow of the American Academy of Arts and Sciences, the American Association for the Advancement of Science, the Geological Society of America, and the American Geophysical Union, where she served as president of the Planetary Sciences Section. In 2013, President Obama appointed Prof. Zuber to the National Science Board.